Journal of Innovative Technology, Vol. 4, No. 1, pp. 33-37, March 2022
http://doi.org/10.29424/JIT.202203_4(1).0006

CFD Study on Settling and Deformation Characteristics of Spherical and Spheroid Newtonian Droplets

Anjani Ravi Kiran Gollakota [1*]

ABSTRACT

Multiphase flows especially Newtonian fluids are extremely widespread in the chemical, biological, petroleum, and polymer processing sectors. Thus, the rise/fall and deformation properties of droplets in immiscible continuous phase solutions are required for the design of multiphase flow equipment. Among the various hydrodynamic properties, drag coefficient plays a vital role in designing contacting equipment. In the present study, the rheological aspects of settling and deforming both spherical and non-spherical droplets in stagnant air were analyzed through computational fluid dynamics solver COMSOL Multiphysics 4.3. Further, continuous phase was selected as Newtonian medium (air) and the dispersed droplet phase consisting of Newtonian fluids (water). Volume fraction images of spherical and spheroid droplets demonstrate substantial distortion in the initial stages, with the tendency to deform gradually decreasing as the droplet approaches the channel's bottom. The drag coefficient of a moving droplet is determined in relation to time in order to comprehend the deformed Newtonian droplets' settling velocity behavior. Additionally, the volume fraction contours, pressure contours, and drag distributions of settling droplets are presented in detail to indicate the mixing behavior.

Keywords: Newtonian fluids, droplets, two-phase flow, drag coefficient, spheroid

1. INTRODUCTION

The rheology of emulsions (where one fluid is dispersed into another) and transport phenomena, droplet deformation, and terminal velocity are critical considerations in chemical process engineering industries. The rise or fall of droplets in rheological simple and complex fluids is also crucial in dealing with the hydrodynamics of fermenters, mixing, and separation processes. Further, equipment's physical properties cannot be predicted unless the interactions between irregular particles and the surrounding fluids are clearly known. Gas-liquid reactors with unsteady, scattered gas flows have been modeled numerically using Euler/Euler and Euler/Lagrange methods developed over the last decade (Gollakota and Kishore, 2017). In both of these methods, the source term is the sum of all the forces between the two phases. This source term is used to account for the movement of momentum between the two phases. Numerous studies have been conducted under the assumption that droplets are spherical, which is true for small droplets but not true for bigger droplets. While treating an irregular body computationally using a conventional Cartesian, cylindrical polar, or spherical polar coordinate system is more difficult, numerical procedures for solving the full Navier-Stokes equation on non-orthogonal boundary fitted coordinates have been practiced for several decades (Gollakota and Kishore, 2015). Modern computers are capable of solving the whole Navier-Stokes equation, allowing for numerical simulations of separated flows past non-spherical objects. Masliyah and Epstein (1971), for instance, conducted a numerical investigation of flow past a hard spheroid. The Navier-Stokes equation is translated into a vorticity-stream function formulation based on spheroidal coordinates to correspond to the spheroid boundary condition and then discretized using the finite difference approach in their study. There has been considerable research on the rise and fall of liquid drops in Newtonian media, as well as the fall of a solid sphere in a rectangular chamber through Newtonian and non-Newtonian fluids (Wanchoo et al., 2003; Astarita & Appuzzo, 1965; Calderbank et al., 1970; Acharya et al., 1977; Acharya et al., 1978). Taylor and Acrivos, (1964) investigated the deformation of a non-buoyant slender droplet embedded in a simple extensional flow of a Newtonian liquid and discovered that the droplet achieves a parabolic shape with pointed ends. According to Garner and Hammerton, (1954), distortion and oscillation of the drop will affect the drag coefficient, which will cause the terminal velocity across the rigid sphere of equal volume to decrease. Using this equation $\frac{v^2}{r} = \frac{a}{\rho}$ Hermann was able to figure out the final velocities of water droplets. The equation says that where is the settling velocity, r is the radius of a spherical drop with the same mass as the actual drop, and is the air density. The coefficient is based on the drag coefficient of the spherical drop and its diameter. Through volume simulations, (Rabha & Buwa, 2010) investigated lift forces acting on single or multiple droplets in linear shear flow. They found that for a highly viscous system, the value of lift coefficient is linear with the horizontal Eötvös number, but for a low viscous system, the droplet tends to fluctuate values of lift coefficient, which increases with the droplet's diameter. However, very limited information is available

Manuscript received March 7, 2022; revised March 22, 2022; accepted March 22, 2022.

[1*] Assistant Professor (corresponding author), Department of Safety, Health and Environmental Engineering, National Yunlin University of Science and Technology, Taiwan (ROC). (email: gollakota.iitg@gmail.com)

about the shape and deformation of Newtonian droplets of various shapes such as sphere, prolate spheroid, and oblate spheroid that lie within Newtonian domains. With advancements in numerical methods, which have become the most efficient approaches with some useful advantages for understanding the transport phenomena and hydrodynamics of droplets, commercial software based on CFD can be used to obtain information on the shear rate dependence of the viscosity and stress field. Thus, the purpose of this work is to present numerical data on the settling and deformation phenomena of Newtonian spherical and spheroidal droplets.

2. PROBLEM STATEMENT AND MATHEMATICAL DESCRIPTION

To investigate spherical deformation, oblate and prolate droplets are allowed to settle in a warm air chamber. Newtonian droplets are water and air. Table 1 shows the fluid characteristics. The droplet is 0.1 times the chamber's width. As illustrated in Figure 1, the droplets fall freely from 18.5 m above the channel's top. The constant phase remains static. The problem is regulated by the phase continuity and momentum equations. continuity equations as follows:

Continuity equation:

$$\nabla \cdot V = 0$$

Momentum Equation:

$$\rho\left[\left(V \cdot \nabla\right)V\right] = -\nabla P + \nabla \cdot \tau$$

Extra stress tensor can be written as**:**

$$\tau = 2\eta\varepsilon$$

Drag coefficient:

$$C_d = \frac{2F_d}{\rho\mu^2 A}$$

Table 1. Properties of Continuous and discontinuous phases

Material	ρ (kg/m^3)	n	λ(s)	μ_0 (kg/m.s)	μ_∞ (kg/m.s)	Simulation Time
Newtonian						
Air	1.2	-	-	-	-	0 - 2 Sec
Water	1000	-	-	-	-	0 – 2 Sec

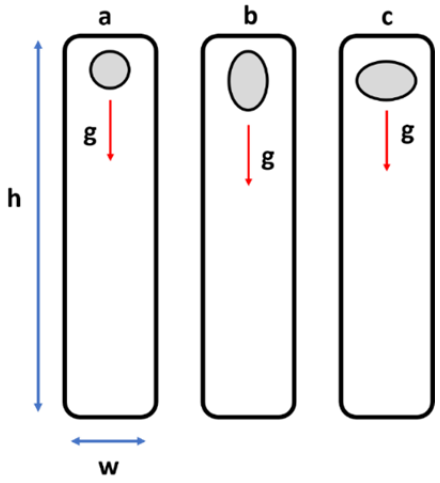

Fig. 1 (a) Computational domain for the spherical droplet in the stagnant air medium, (b) Oblate spheroid droplet in the stagnant air medium, (c) Prolate spheroid droplet in the stagnant air medium

3. NUMERICAL METHODOLOGY

Comsol Multiphysics 4.3 was used to solve the governing equations and boundary conditions. Simulating each element size at 0.28 m, 0.04 m, and 1.1 m takes roughly 25-30 minutes with fine meshing to produce good convergence and correct solutions. The simulations were run in the time range (0 – 2 sec) using a time step of 0.1 sec. The Lagrange P2P1 method is used to approximate the pressure values. The inputs are chosen so that the continuous phase density and viscosity are constant. For symmetric and non-symmetric systems, Comsol employs the PARDISO solver, which has failed to attain the needed level of convergence. Simulations were run at various time stages. The present study uses a time-dependent solver to estimate the drop's velocity and deformation at 0.1sec inside a channel where time is controlled rather than location. The grid and domain employed in this study are not further studied because the effects of the wall are not examined. Hence, the fine mesh with 12000 node points was selected in the present study.

4. RESULTS AND DISCUSSION

4.1 Validation using Comsol 4.3

Validation of numerical solutions with existing experimental and/or numerical data is required for reliability and accuracy. The container's height and diameter are the same as Ismail, (2007). Ismail, (2007) investigated the problem of a submerged oil bubble rising in water, which is heavier than oil. The simulation conditions for the validation studies were similar to the case of Ismail, 2007. No external force is given to the bubble, and the buoyancy force causes the scattered phase to migrate into the continuous phase. The containers' top and bottom are non-slip, but the vertical sides are wetted to facilitate fluid interface movement. Figure 2 compares the modeling results to Ismail's experimental results. This increases our solver's confidence and allows us to analyze droplet deformation without dispersion in stationary air.

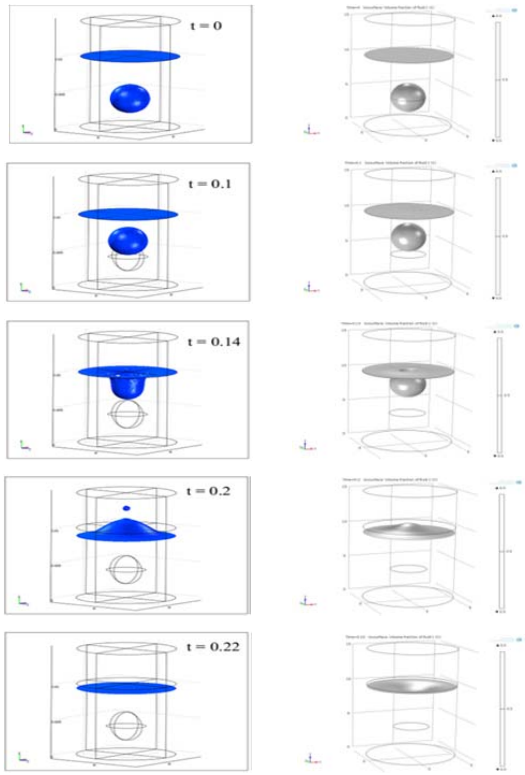

Fig. 2 Comparison of Volume fraction images of Oil bubble rising in water observed in (Ismail, 2007) and the present predictions

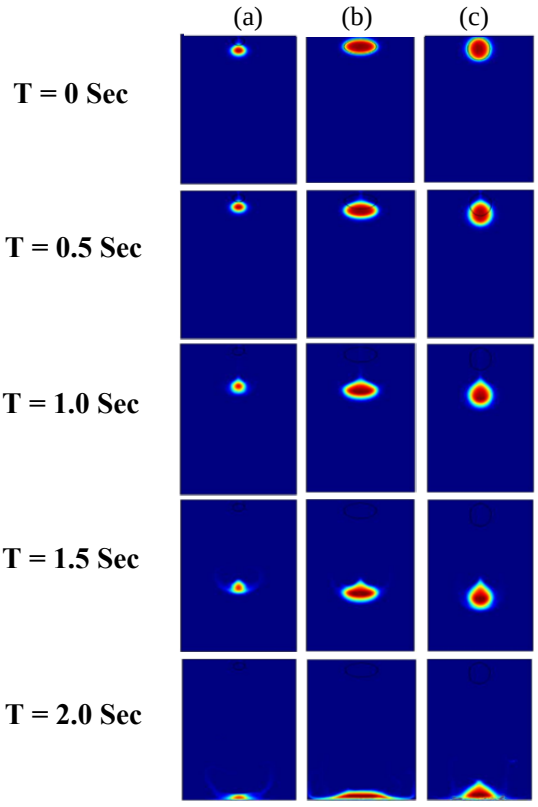

Fig. 3 Volume fraction of spherical and spheroidal Newtonian droplets settling in stagnant air a) Spherical b) Oblate ellipsoid c) prolate ellipsoid

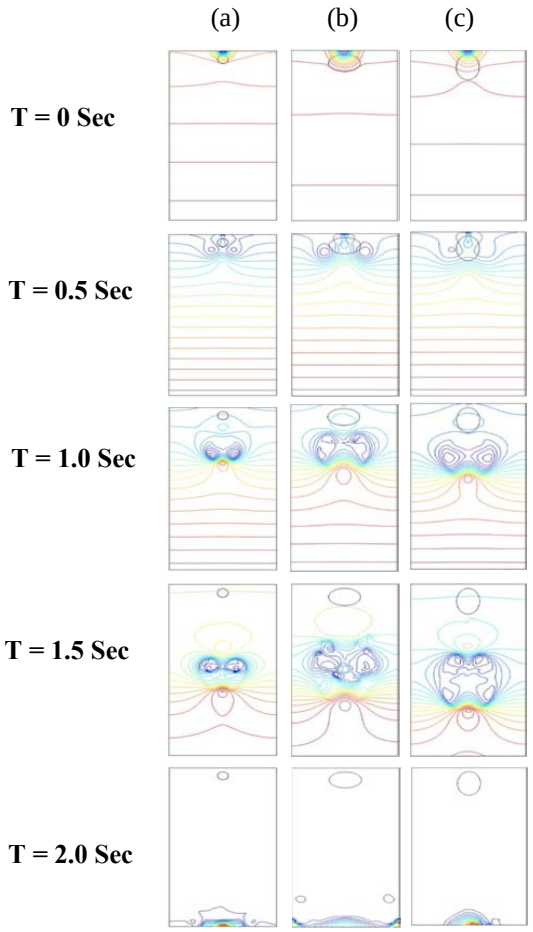

Fig. 4 Pressure Distribution of spherical and spheroidal Newtonian droplets settling in stagnant air a) Spherical b) Oblate ellipsoid c) prolate ellipsoid

4.2 Volume fraction studies

Clift et al., (1978) categorized free-moving bubbles and drops as spherical, ellipsoidal, or spherical cap or ellipsoidal. Interfacial and viscous forces dominate inertial forces in spherical droplets and bubbles. Oblate with the convex surface, the drips and bubbles are ellipsoidal. Spherical or ellipsoidal cap: These are the largest droplets or bubbles that are flat dimpled or skirted at the back. When exposed to external flow fields, the drop deforms until normal and shear stresses balance. Larger deformations occur when interfacial forces exceed viscous forces, and undeformed when viscous forces exceed inertial forces. Aside from the continuous phase's physical features, restricting walls influence the morphology of drops, especially bubbles Coutanceau and Thizon, (1954). Without consideration of wall effects, the forms of bubbles and droplets rising or falling freely in a liquid medium are determined by the magnitudes of the dimensionless Reynolds number factors. The goal of these deformation studies is to demonstrate visually that the simulation technique accurately reproduces the gross effects of interfacial and hydrodynamic interactions, while quantitative data from experimental research are not easily available.

The volume fraction of Newtonian droplets settling in stagnant air is plotted in Figure 3 as spherical (Figure 3(a)), oblate (Figure 3(b)), and prolate (Figure 3(c)) droplets. When a droplet falls freely from the channel's top (19.5 m above the bottom surface seen in Figure.1), the time interval required for

the droplet to deform is (0 - 2 sec). At t=0, the shape of the droplet with radius r - 0.5m is precisely spherical due to the fact that surface tension seeks to reduce the droplet's surface area, so forming a sphere. At time t = 0, the droplet is assumed to be stationary, with an initial velocity of zero. The droplet moves primarily as a result of the density differential between the scattered and continuous phases, as well as the downward pull of gravity. Unless the density difference is quite large, it is found that the falling droplet takes a straight route.

Although the droplet deforms early, no significant deformation is detected between 0 and 2 seconds. At t = 0.5, the initially spherical droplet warped into an oblate shape due to the fact that while the droplet settles down due to gravity, opposing forces known as pressure forces created by the surrounding stagnant medium act upward and on the droplet's surface, causing the droplet to deform. Second, as the velocity of the falling drop increases, disturbances in the stagnant surrounding fluid are formed, which adds stress to the drop caused by the disturbances created during settling and causes the drop to deform. However, the surface tension forces at the top of the drop are negligible, and so the bubble's top surface remains spherical, as illustrated in Figure 3(a) for time increments of 2 - 4 seconds. When a little bubble rose in such a fluid, the typical stress acting on the bubble's side caused it to take on a prolate shape. Similar drop deformation tendencies are found in the oblate and prolate spheroids depicted in Figure 3(b), Figure 3(c), and Figure 3(d) (c).

4.3 Pressure distribution studies

The physics underlying the pressure distribution of the droplets are more generally addressed by examining the air and water systems. As illustrated in Figure.4, the only reason for the drop's mechanical stability is due to the surface forces between the fluid and the drop contact. When surface tension acts alone, it succeeds in molding the drop into a shape with a low surface-to-volume ratio. The net inward pull of the molecules deeper within the drop increases the surface tension of the liquid, increasing the pressure within the drop and above the prevailing continuous phase outside the drop.

The current system, as seen in Figure 4, indicates that the water drop is traveling at a terminal velocity, implying that it is being held against gravity by the vertical component of the pressure forces and the surface shear stresses caused by the upward rushing air. Similarly, the drop should have the same vertical pressure gradient as any mass of fluid (air) at rest in a gravitational field. Internal recirculation within the drop, as illustrated in Figure 4, can be explained as if the barrier of an air flow were solid. The no-slip boundary condition asserts that air is in contact with a reasonably still border. When a water drop falls in air as a continuous medium, the no-slip boundary condition ensures that the air surface moves slowly enough for the interfacial liquid to drift downstream at the same rate as the air, and thus these recirculations occur as a result of the shear stress exerted by the ambient air. Qualitatively, one can state that a very small amount of internal recirculation is unavoidable for the dynamic boundary condition due to the continuity of the tangential sear stresses across the water air interface, and additionally, because water viscosity is not infinite, some amount of internal motion appears certain to develop.

4.4 Drag Coefficient and Time Graphs

The forces acting on the droplet define its mobility and kinetics. The forces acting on freely and steadily descending particles are the particle's downward force due to its own weight. The normal and tangential forces act in the opposite direction to the particle's weight. It is well known that taking the integral over the normal force's surface results in the buoyancy force, which is independent of the particle's shape. Among the many forces, one that must be considered is the drag force acting on the descent. The drag coefficient is typically used to quantify an object's resistance in a fluid environment such as air or water. The motion of a liquid drop or a gas bubble is unlike that of a spherical particle of equal mass and volume. The liquid passing past the drop causes friction, which results in the formation of the droplet's circulations. Additionally, as the drop descends, forces caused by pressure non-uniformity act on the drop surface, distorting the drop's spherical shape. These forces are resisted by the surface tension forces, which retain the drop's spherical shape. The drag coefficient is derived using the equation $C_d = 4 \times d \times g \frac{(\rho_l - \rho_g)}{3 \times \rho_l \times (v)^2}$ where d is the diameter of the droplet, g is acceleration due to gravity is the density of the droplet (dispersed phase), is the density of the air (continuous phase), and is the droplet's velocity. The eccentricities of the droplets are denoted by the constant e, which is determined using the spheroids' major and minor axes. The main and minor axes are defined as follows: the axis perpendicular to the flow direction is called the minor axis, and the axis parallel to the flow direction is called the major axis. The drag coefficient is plotted against the time relationship for Newtonian and non-Newtonian droplets falling freely in stagnant air functioning as a continuous medium in Figure.5, As the duration of settling rises, the corresponding terminal settling velocities of the droplets increase due to the droplet becoming completely free under the effect of gravity. As a result, the drag coefficient of the vehicle is reduced. In conclusion, the drag coefficient lowers as the velocity increases, which increases the Reynolds number; as the Reynolds number grows, inertial forces outweigh viscous forces, and therefore the drag coefficient drops.

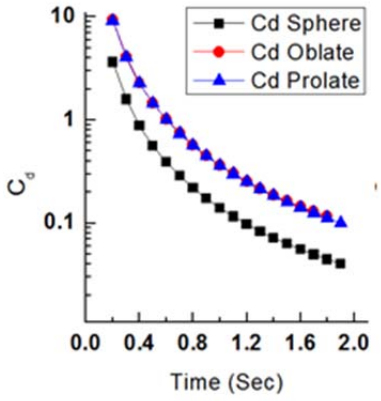

Fig. 5 Drag Coefficient Vs Time Graphs for both spherical and non-spherical droplets deforming in Newtonian medium

5. CONCLUSIONS

In this work, different aspects of falling droplet movement shape of the droplet while falling, the terminal velocity of the droplet, and the drag coefficient of spherical, oblate spheroid, and prolate spheroid droplets are determined. Numerical studies cover droplets of different shapes and velocities at different time steps ranging from 0-2 sec. It is recognized that drop deformation occurs as a result of the viscous forces of the surrounding liquid, external disturbances caused by wall effects, and dimensionless characteristics such as the Reynolds number, weber number, and Bond number, among other. From the outlines of the velocity distribution, it is noted that the velocity steadily increases as it falls freely and achieves a nearly constant value before colliding with the channel's bottom surface. In the simulation, no separate inlet velocity is applied to cause the droplet to migrate. Additionally, it is noticed that the velocity variation with respect to the varied fluid characteristics appears to be approximately similar, as does the deformation of the various droplets. It is noted from the drag coefficient vs. time plots that as time passes, the drag coefficient reduces due to the rise in velocity, but the velocity abruptly decreases as it reaches the bottom surface.

References

Acharya, A., Mashelkar, R. A., & Ulbrecht, J. (1977). "Mechanics of bubble motion and deformation in non-Newtonian media." *Chemical Engineering Science*, **32**(8), 863-872.

Acharya, A., Mashelkar, R. A., & Ulbrecht, J. (1978). "Motion of liquid drops in rheologically complex fluids." *The Canadian Journal of Chemical Engineering*, *56*(1), 19-25.

Astarita, G., & Apuzzo, G. (1965). "Motion of gas bubbles in non-Newtonian liquids." *AIChE Journal*, **11**(5), 815-820.

Calderbank, P. H., Johnson, D. S. L., & Loudon, J. (1970). "Mechanics and mass transfer of single bubbles in free rise through some Newtonian and non-Newtonian liquids." *Chemical Engineering Science*, **25**(2), 235-256.

Clift, R. Grace, J.R., Weber, M.E. (1978). *Bubbles Drops and Particles. Academic Press. New York.*

Coutanceau, M., & Thizon, P. (1981). "Wall effect on the bubble behaviour in highly viscous liquids." *Journal of Fluid Mechanics*, *107*, 339-373.

Garner, F. H., & Hammerton, D. (1954). "Circulation inside gas bubbles." *Chemical Engineering Science*, **3**(1), 1-11.

Gollakota, A. R. K., & Kishore, N. (2015). "A numerical study on flow and drag phenomena of spheroid bubbles in Newtonian and shear-thinning power-law fluids." *International Journal of Modelling and Simulation*, **35**(2), 73-81.

Gollakota, A. R., & Kishore, N. (2018). "CFD study on rise and deformation characteristics of buoyancy-driven spheroid bubbles in stagnant Carreau model non-Newtonian fluids." *Theoretical and Computational Fluid Dynamics*, **32**(1), 35-46.

Ismail, M. (2007). "Level-Set and phase field methods: Application to moving interfaces and two-phase fluid flows". *Scientific computing.*

Masliyah, J. H., & Epstein, N. (1971). "Steady symmetric flow past elliptical cylinders." *Industrial & Engineering Chemistry Fundamentals*, **10**(2), 293-299.

Rabha, S. S., & Buwa, V. V. (2010). "Volume-of-fluid (VOF) simulations of rise of single/multiple bubbles in sheared liquids." *Chemical Engineering Science*, **65**(1), 527-537.

Taylor, T. D., & Acrivos, A. (1964). "On the deformation and drag of a falling viscous drop at low Reynolds number." *Journal of Fluid Mechanics*, **18**(3), 466-476.

Wanchoo, R. K., Sharma, S. K., & Gupta, R. (2003). "Shape of a Newtonian liquid drop moving through an immiscible quiescent non-Newtonian liquid." *Chemical Engineering and Processing: Process Intensification*, **42**(5), 387-393.